

# EXPERIMENTAL STUDY AND IMAGE PROCESSING-BASED MEASUREMENT OF SPRAY BREAKUP LENGTH IN MICROTURBINE VAPORIZER TUBES

Huu Ha Nguyen<sup>1,\*</sup>, Quoc Quan Nguyen<sup>1</sup>, Xuan Phuong Pham<sup>1</sup>

<sup>1</sup>*Institute of Vehicle and Energy Engineering, Le Quy Don Technical University*

## Abstract

Measuring spray breakup length is a critical requirement for optimizing vaporizer tube design in microturbines. High-speed photography is a widely used modern measurement technique; however, its application in vaporizer tubes requires accurate image processing algorithms to account for light refraction through quartz tube walls and noise from fuel density variations. This study develops an algorithm that combines adaptive thresholding with Sobel edge detection, optimized for the vaporizer tube environment. Experiments were conducted at injection pressures ranging from 1.38 to 4.14 bar, with more than 4000 images analyzed per condition to ensure statistical reliability. The results show that breakup length increases from 3.2 mm to 6.8 mm as injection pressure rises, with clear periodic oscillations observed. The algorithm achieves an accuracy of  $\pm 0.01$  mm with full automation, providing an effective tool for research on vaporizer tube optimization in microturbines.

**Keywords:** Vaporizer; image processing; breakup length; Sobel operation; OpenCV.

## 1. Introduction

Microturbines are widely used in unmanned aerial vehicle (UAV) systems and industrial applications due to their compact size and high power-to-weight ratio [1], [2]. However, optimizing combustion performance in small-scale combustors presents significant challenges, particularly due to space constraints and high-performance requirements.

In these combustors, vaporizer tubes serve as the primary fuel preparation device, functioning to convert liquid fuel into vapor and create a mixture with air prior to combustion. Due to size and weight constraints, vaporizer tubes are often the only option for microturbine engines, replacing the more complex fuel injection systems used in larger engines [3].

The fuel spray breakup process within vaporizer tubes plays a critical role in creating homogeneous fuel-air mixtures, directly affecting combustion efficiency, emissions, and engine stability. Developing accurate measurement methods for spray breakup processes is essential to support combustor design optimization, improve combustion stability, and reduce emissions [3].

---

\* Corresponding author, email: huuha84@lqdtu.edu.vn  
DOI: 10.56651/lqdtu.jst.v21.n1.1034

This study develops advanced image processing algorithms to accurately measure spray breakup length in microturbine vaporizer tubes, combined with experimental systems that simulate actual fuel injection conditions. The objective is to provide tools and experimental data to improve combustion performance and engine durability.

## 2. Theoretical background and spray measurement methods

### 2.1. Spray breakup theory in vaporizer tubes

Microturbines utilize annular combustors with fuel injectors located at the inlet of vaporizer tubes (Fig. 1) [4]. Fuel is injected coaxially with the airflow, undergoing spray breakup, vaporization, and mixing before entering the combustion zone [5]. Vaporizer tubes play a critical role, with their geometry and injector positioning carefully designed to ensure fuel-air mixture quality. Waitz *et al.* [4] identified key design constraints for small-scale combustors, emphasizing the importance of fuel preparation processes within confined spaces.

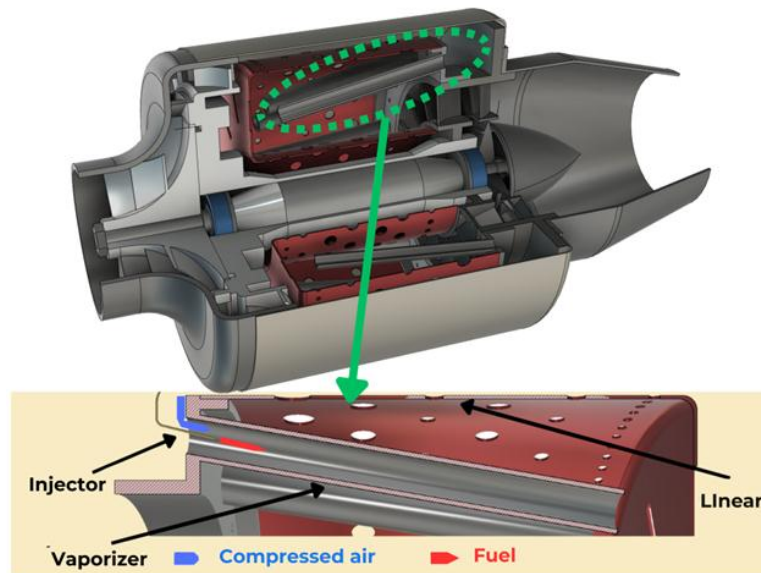


Fig. 1. The position of the vaporizer tubes and injectors in the combustor.

The spray breakup process occurs through two stages: primary breakup, where the continuous fuel jet experiences shear forces from the coaxial airflow, combined with viscosity and surface tension effects to break into ligaments and large droplets [6]-[8]; and secondary breakup, where large droplets continue to fragment, increasing surface area and promoting vaporization (Fig. 2) [9]. Parameters such as injection pressure, coaxial air velocity, fuel viscosity, and surface tension significantly influence this process. Faeth *et al.* [10] demonstrated that high pressure and high air velocity increase shear forces, reducing breakup length and droplet size.

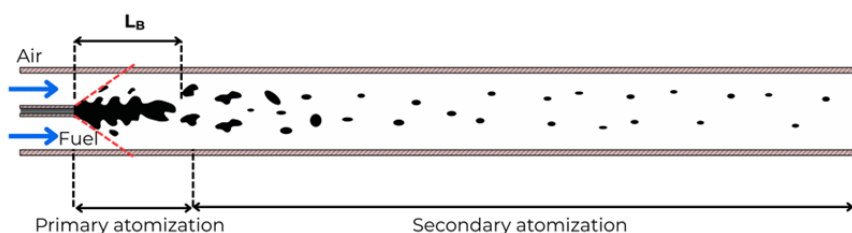


Fig. 2. The spray breakup process in the vaporizer tubes [9].

Current research on vaporizer tubes primarily focuses on overall flow patterns and heat transfer, while spray breakup mechanisms, which are the core process determining mixture quality, have not received proportional attention. Works by Velidi and Yoo [2] as well as Large and Pesyridis [1] identify combustor optimization as the primary challenge but do not delve deeply into spray breakup mechanisms under the specific conditions of vaporizer tubes. The breakup length, defined as the distance from the injector tip to the point where the fuel jet transitions into droplets, is a critical design parameter that directly affects combustion performance and requires more detailed investigation [10]-[13].

## 2.2. Spray breakup length measurement methods

Breakup length ( $L_b$ ) is defined as the distance from the injector tip to the point where the continuous fuel jet transitions into a discrete two-phase flow [14]. Three main categories of measurement methods have been developed: intrusive methods using physical probes [15], advanced optical techniques such as laser-induced fluorescence (LIF) [16], and direct optical imaging [17]. Intrusive methods offer high accuracy but are unsuitable for small-diameter vaporizer tubes due to flow disturbance. LIF techniques provide detailed information but require complex equipment, high costs, and specialized tracer materials.

Shadowgraphy has become the dominant method in modern spray research. This technique uses high-speed cameras to capture spray silhouettes through backlighting, enabling direct, non-intrusive observation of breakup processes [18]. Advantages include reasonable cost, high flexibility, real-time analysis capability, and no requirement for tracer materials. Sommerfeld and Qiu [13] confirmed the effectiveness of this method in complex spray studies.

However, applying shadowgraphy in microturbine vaporizer tubes presents specific challenges: light refraction and scattering through quartz tube walls reduces contrast, fuel density gradients create dynamic optical noise, and uneven illumination occurs due to space constraints. To ensure statistical reliability, large volumes of data

must be processed with high accuracy. These challenges require developing image processing algorithms specifically optimized for shadowgraphy in vaporizer tubes, combining adaptive thresholding and edge detection.

### **2.3. Image processing techniques in spray measurement**

The effectiveness of shadowgraphy techniques depends entirely on the quality of image processing algorithms. Basic algorithms comprise two main groups: image segmentation techniques (fixed and adaptive thresholding) and edge detection operators (Sobel, Canny, Prewitt) [18]. Adaptive thresholding is particularly effective under non-uniform illumination and high noise conditions, while the Sobel operator is suitable for environments with low signal-to-noise ratios [19]. Research by Saini and Biswas [20] demonstrated the superior effectiveness of combining adaptive thresholding with edge detection in underwater environments, sharing many characteristics with vaporizer tubes regarding light refraction, density gradients creating optical noise, and non-uniform illumination (Fig. 3). Roy *et al.* [21] also confirmed the advantages of adaptive thresholding in processing images with varying optical characteristics.

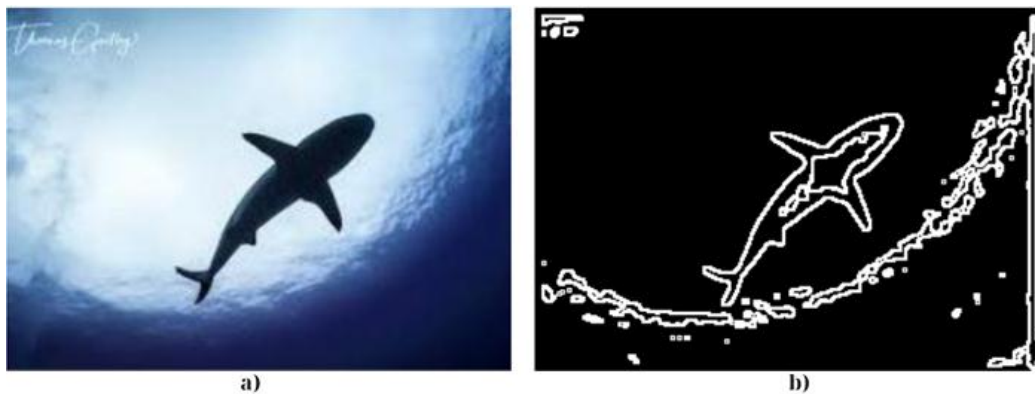


*Fig. 3. Method combining adaptive thresholding and Sobel operator [22]:  
a) Raw image; b) Processed image.*

However, the application of image processing for spray measurement in microturbine vaporizer tubes remains underexplored. Current research primarily focuses on free jet spray environments with simpler optical conditions, while vaporizer tubes present specific challenges that have not been systematically addressed. No studies have developed optimized algorithms for processing light refraction through curved quartz tube walls, compensating for image distortion from circular tube geometry, and adapting to fuel density gradients within confined spaces. This gap creates a need for developing advanced image processing algorithms specifically designed for the unique conditions of vaporizer tubes.

### 2.4. Research gap

Shadowgraphy has become the dominant method in spray measurement due to its non-intrusive nature and reasonable cost. However, using this technique to study spray breakup processes in microturbine vaporizer tubes faces specific challenges. Primary challenges include light refraction through quartz tube walls, optical noise from fuel density gradients, and the requirement to process large volumes of data to ensure statistical reliability. Currently, no image processing algorithms have been specifically optimized for these conditions, while vaporizer tube research primarily focuses on flow patterns and heat transfer rather than delving into spray breakup mechanisms. These challenges create a need to develop image processing algorithms specifically designed for vaporizer tube research, combined with experimental systems that simulate actual operating conditions.

## 3. Experimental setup and methodology

### 3.1. Experimental system design

The experimental system was designed to investigate spray breakup processes in microturbine vaporizer tubes, with the objective of accurately replicating actual fuel injection conditions. The system comprises four main subsystems: (1) liquid supply system, (2) compressed air supply system, (3) experimental combustor, and (4) image acquisition system. The overall schematic is presented in Fig. 4, while the laboratory equipment arrangement is shown in Fig. 5.

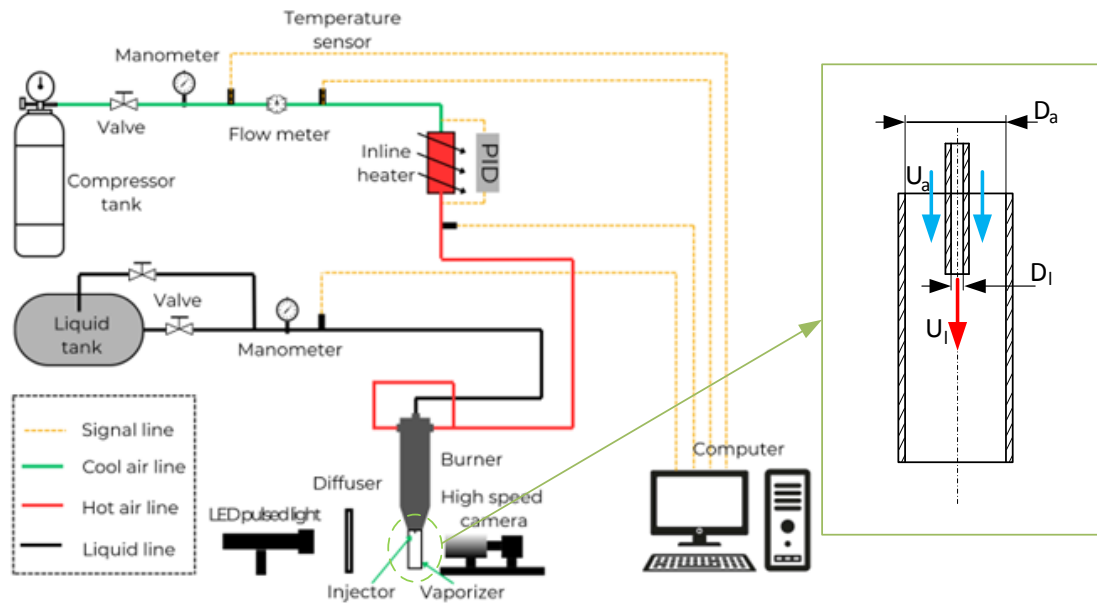
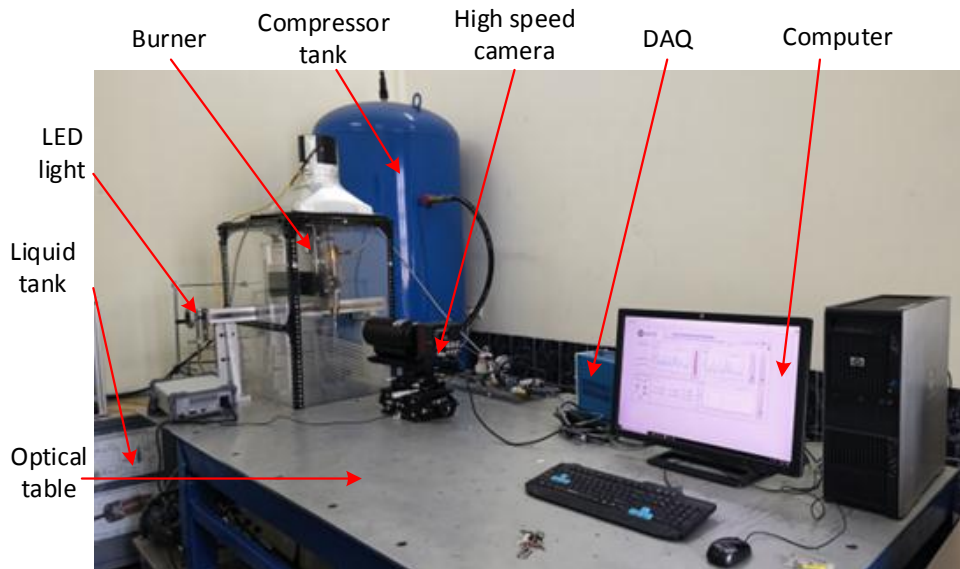


Fig. 4. Schematic of the experimental system.

The experimental burner was designed based on the Sydney Burner prototype [23], with geometric parameters adjusted to match Jetcat P130RX microturbine vaporizer tubes. This enables accurate simulation of the flow environment and thermodynamic conditions in practical applications. To enable optical observation, the metallic vaporizer tube was replaced with a quartz tube having identical geometric dimensions, ensuring high optical transparency and minimizing refraction effects that could affect image quality. Table 1 presents the main technical specifications of the vaporizer tube and injector used in this spray breakup study.

*Tab. 1. Main technical specifications of the experimental system*

Parameters	Value
Inner diameter of the vaporizer tube, (mm)	5
Inner diameter of the injector, (mm)	0.21
Outer diameter of the injector, (mm)	0.4
Camera frame rate, (frames/second)	5000
LED pulse frequency, (Hz)	5000



*Fig. 5. System arrangement in the laboratory.*

Pressure and flow sensors were installed at appropriate locations on the liquid and compressed air supply lines to continuously monitor key operating parameters, including injection pressure and coaxial air velocity. Data from these sensors were used

for experimental control and results analysis. Electronic pressure regulators and SMC linear valves, combined with PID temperature control systems, were employed to maintain stable operating conditions, ensuring that injection pressure and experimental ambient temperature remained within required ranges, thereby ensuring repeatability and reliability of spray breakup length measurements.

The illumination system employed high-intensity pulsed LED techniques, precisely synchronized with the high-speed camera to achieve image ‘freezing’ at extremely short exposure times ( $< 1 \mu\text{s}$ ). This approach allowed the capture of rapid spray dynamics with high sharpness while minimizing motion blur. The Photon FASTCAM Mini AX100 high-speed camera, which is capable of recording up to 200,000 frames per second, was operated at 10,000-20,000 fps in this study to ensure sufficient spatial resolution for detailed spray structure analysis and accurate breakup length determination.

The spatial configuration of the system was optimized to ensure precise coaxial alignment between the injector and air flow, while creating optimal observation conditions within the quartz vaporizer tube. This integrated design enables accurate reproduction and tight control of fuel injection conditions characteristic of small gas turbine engines. The system ensures acquisition of high-quality image data, providing a reliable foundation for developing and validating image processing algorithms aimed at determining spray breakup length.

### ***3.2. Data acquisition procedure***

The experimental operating procedure was conducted under specific operating conditions to accurately simulate fuel injection conditions in microturbine vaporizer tubes. Based on combustor simulation results for the Jetcat P130RX engine, vaporizer tube operating parameters were determined with fuel injection pressures ranging from 1.38 to 4.14 bar and coaxial air flow rate of 100 L/min, aimed at reproducing representative operating conditions of this microturbine [24]. Specific test conditions are presented in Tab. 2, including dimensionless Weber (We) and Reynolds (Re) numbers to characterize the spray breakup regime.

The experimental ambient temperature was maintained stable at  $25^{\circ}\text{C} \pm 1^{\circ}\text{C}$  using a PID temperature control system, ensuring that the physical properties of the test liquid did not change significantly during measurements. Prior to each experiment, the system was operated for 10 minutes to achieve steady flow conditions and eliminate startup effects.

For each experimental condition, a minimum of 5,000 frames were continuously acquired to ensure statistical representativeness of the data. Images were stored in uncompressed format to preserve original quality for processing. After acquisition, images were filtered based on quality criteria including sharpness, contrast, and noise levels. Only images meeting quality standards were included in the analysis, with valid image rates typically exceeding 95%.

*Tab. 2. Experimental operating conditions*

Cases	Air flow rate (L/min)	Injection pressure (Bar)	$U_a$ (m/s)	$U_l$ (m/s)	$Re_l$	$We_g$
1	100	1.38	85	5	2897	4.91
2	100	2.12	85	6.2	2897	5.17
3	100	3.14	85	7.5	2897	7.34
4	100	4.14	85	8.6	2897	9.89

System calibration was performed before each experimental session, including pixel/mm ratio calibration using calibration targets and verification of injector alignment. Calibration accuracy reached  $\pm 2 \mu\text{m}$ , ensuring high reliability for spray breakup length measurements. The entire data acquisition procedure was automated through control software, minimizing human error and enhancing experimental repeatability.

### **3.3. Image processing algorithm**

The image processing procedure was specifically developed for vaporizer tube conditions, combining adaptive thresholding and Sobel edge detection operators to accurately extract spray boundaries and measure breakup length from thousands of high-speed images. The algorithm was optimized to handle specific challenges of the vaporizer tube environment including light refraction through quartz tube walls, liquid density gradients, and non-uniform illumination. The processing procedure is illustrated in Fig. 6.

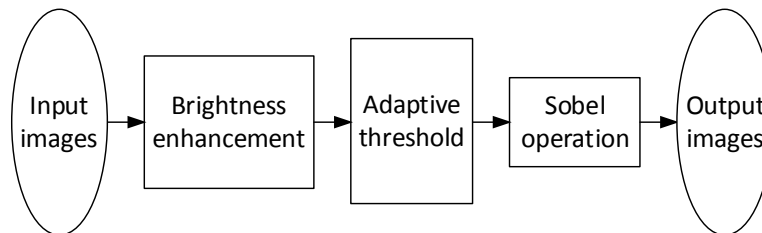


*Fig. 6. Image processing workflow.*

The preprocessing stage aims to improve the quality of raw images affected by optical effects within the vaporizer tube. Original images typically exhibit low contrast due to light refraction and scattering through curved quartz tube walls, accompanied by noise from liquid density gradients. Adaptive histogram equalization contrast enhancement techniques were applied in combination with Gaussian filtering to reduce noise while preserving important spray details. Mathematically, this process is represented by Eq. (1) [18]:

$$I'(x, y) = \frac{I(x, y) - I_{\min}}{I_{\max} - I_{\min}} d_r + I_0 \quad (1)$$

where  $I(x, y)$  is the intensity value at pixel  $(x, y)$ ,  $I_{\min}$  and  $I_{\max}$  are the minimum and maximum intensities in the original image, respectively,  $d_r$  is the dynamic range scaling factor,  $I_0$  is the offset value, and  $I'(x, y)$  is the pixel intensity after normalization.

Image segmentation employs Gaussian adaptive thresholding techniques to address the characteristic non-uniform illumination problem in vaporizer tubes. This method calculates local thresholds for each pixel based on weighted average values of the neighboring region, enabling accurate separation of spray regions from the background even under varying lighting conditions. The threshold at each pixel is determined according to Eq. (2), where the neighborhood window size and correction constant are optimized through experimentation [21],

$$Th(x, y) = Av(x, y) - p \quad (2)$$

where  $Th(x, y)$  is the threshold at pixel  $(x, y)$ ,  $Av(x, y)$  denotes the local average intensity around pixel  $(x, y)$ , and  $p$  is a bias parameter used to adjust the threshold value.

Edge detection applies the Sobel operator, which was selected for its effective performance in environments with low signal-to-noise ratios. This operator uses two  $3 \times 3$  kernels ( $H_1, H_2$ ) to calculate gradients in the x and y directions, thereby determining edge intensity and direction [18]. The combined gradient is calculated according to Eq. (3) and (4), enabling identification of spray boundaries with high accuracy even when affected by optical noise,

$$H_1 = \begin{bmatrix} -1 & 0 & 1 \\ -2 & 0 & 2 \\ -1 & 0 & 1 \end{bmatrix}; H_2 = \begin{bmatrix} -1 & -2 & -1 \\ 0 & 0 & 2 \\ 1 & 2 & 1 \end{bmatrix} \quad (3)$$

$$|G| = \sqrt{G_x^2 + G_y^2} \quad (4)$$

where  $|G|$  denotes the gradient magnitude at a pixel,  $G_x$  and  $G_y$  are the gradient components in the horizontal and vertical directions, respectively.

The post-processing stage includes morphological operations to clean up edge detection results. Closing operations are applied to connect discontinuous edge segments caused by noise, followed by area-based filtering to remove small irrelevant objects. The algorithm automatically determines breakup length by finding the farthest point from the injector tip to the location where the continuous fuel jet transitions into discrete droplets. The complete procedure for determining breakup length is illustrated in Fig. 7.

The complete algorithm was implemented using the OpenCV library [25] in Python environment, enabling automated batch processing at approximately 100 images per second on a standard workstation. Algorithm parameters were calibrated using a validation dataset consisting of 500 manually annotated images, achieving an average accuracy of 97.3% compared to ground truth. The high automation capability minimizes subjective errors and enables processing of large data volumes necessary for reliable statistical analysis.

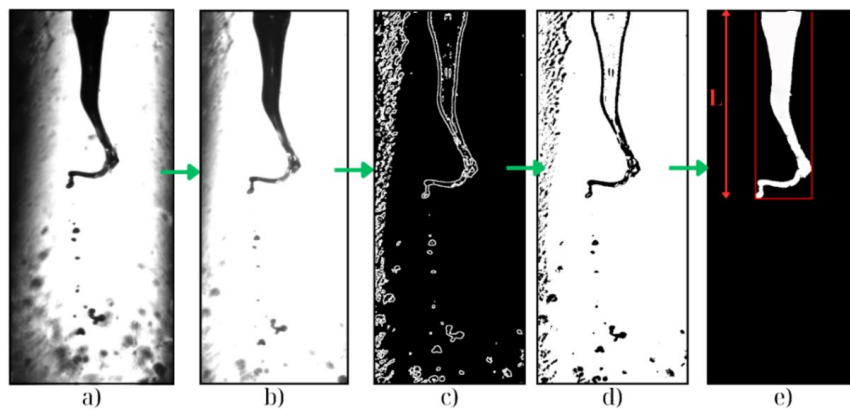


Fig. 7. Image processing to determine breakup length (Case 1):  
 a) Original image; b) Brightness enhancement; c) Binary image;  
 d) Edge detection image; e) Noise filtered image.

### 3.3. Statistical data analysis and processing

Spray breakup length is defined as the distance from the injector tip to the transition point where the continuous fuel jet begins to break up into discrete droplets

and ligaments. This transition point is automatically determined by the algorithm through edge gradient intensity analysis, marking the location where the continuous structure of the fuel jet is disrupted by aerodynamic forces. For each image, breakup length is calculated with pixel-level accuracy, then converted to millimeter units through a predetermined calibration factor.

The dataset obtained from each experimental condition comprises thousands of instantaneous breakup length values, enabling detailed statistical analysis of spray breakup characteristics. The mean breakup length value is calculated as the arithmetic average of all valid measurements under the same operating conditions, accompanied by standard deviation to assess the degree of variation. Breakup length distribution is represented as histograms to observe statistical characteristics, with most cases showing normal distribution with peaks concentrated around the mean value as illustrated in Fig. 8.

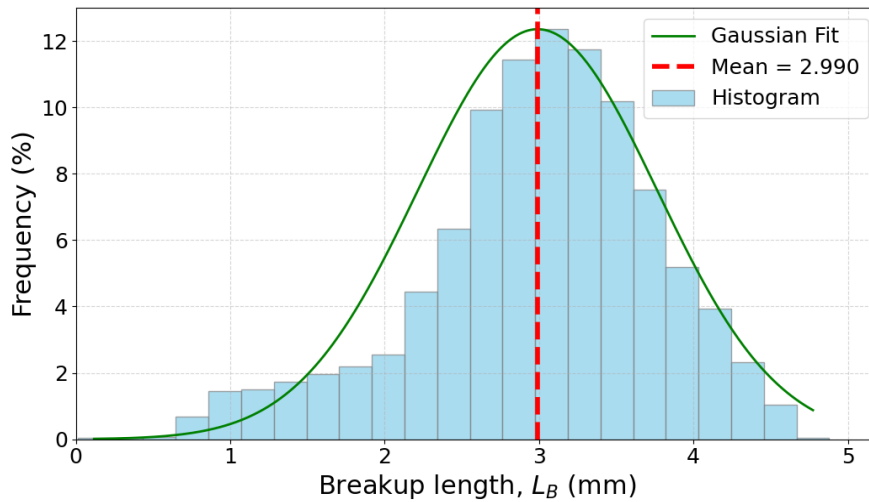


Fig. 8. Breakup length frequency distribution histogram (Case 1).

Time-varying analysis of breakup length was performed through continuous data series, revealing an unstable breakup process with characteristic expansion and contraction cycles. This phenomenon reflects Rayleigh-Plateau instability at the liquid-gas interface, where the fuel jet undergoes gradual downstream elongation until reaching a local instability point ( $t_j$ ), followed by rapid contraction to a new position within time  $t_r$ , as shown in Fig. 9. This breakup-contraction cycle repeats continuously, creating the oscillatory characteristics of breakup length over time.

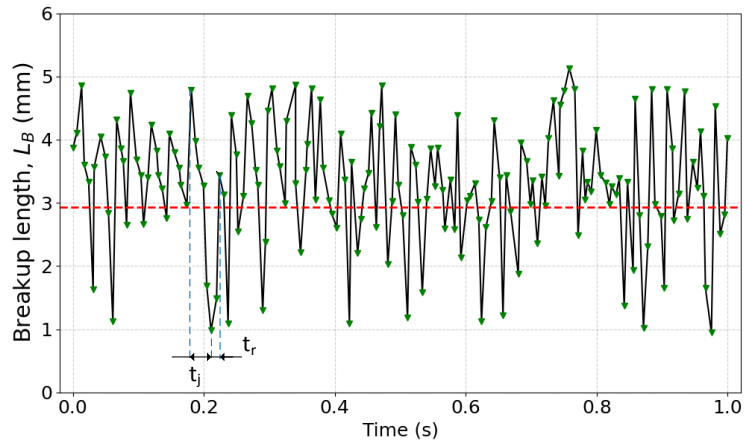


Fig. 9. Spray breakup length fluctuation over time (Case 1).

The statistical reliability of results was evaluated through standard error analysis as a function of sample size. The study shows that standard error decreases following the square-root-n law as the number of images increases, reaching  $\pm 0.025$  mm with 2000 samples,  $\pm 0.018$  mm with 3000 samples, and stabilizing at  $\pm 0.01$  mm when the sample size reaches 4000 images or more as illustrated in Fig. 10. Based on this analysis, a standard procedure was established with a minimum of 4000 images per experimental condition to ensure accuracy and statistical reliability of breakup length measurements.

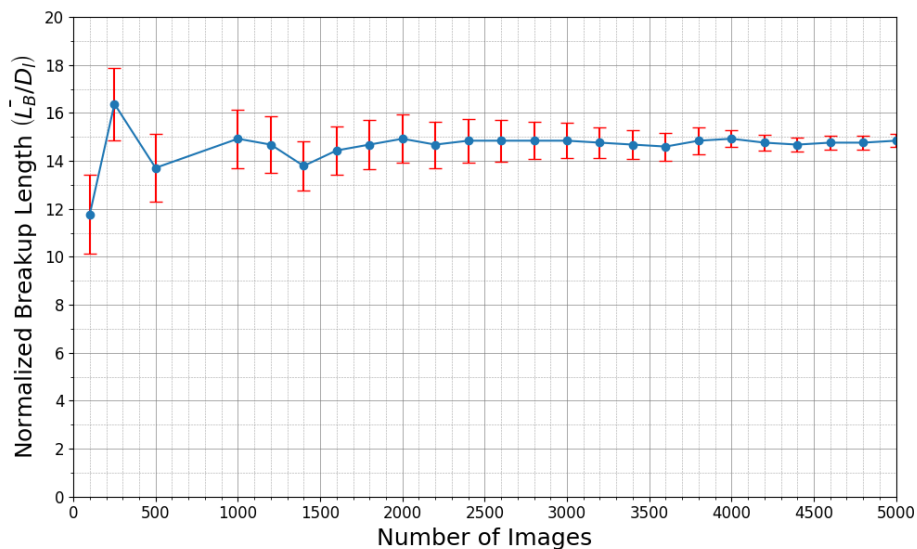


Fig. 10. Normalized breakup length ( $\overline{L_B} / D_1$ ) vs. number of sample images (Case 1).

Detailed statistical analysis was performed using specialized scientific computing libraries. Descriptive statistics such as coefficient of variation (CV), skewness, and

kurtosis were calculated to characterize data distribution. Shapiro-Wilk normality testing was conducted at a significance level of  $\alpha = 0.05$ . One-way analysis of variance and linear regression were applied to evaluate relationships between variables, with results showing strong linear correlation ( $R^2 > 0.95$ ) between injection pressure and mean breakup length.

#### 4. Results and discussion

Experimental results show that spray breakup length in vaporizer tubes increases significantly with injection pressure. Specifically, breakup length varies from 3.2 mm to 6.8 mm as pressure increases within the range of 1.38-4.14 bar (Fig. 11), reflecting the ability to maintain fuel jet continuity before transitioning to discrete droplets.

To enable comparison with other studies, the breakup length was normalized using the expression  $\overline{L_B} / D_l$  where  $\overline{L_B}$  is the mean breakup length and  $D_l$  is the inner diameter of the vaporizer tube. The normalized results increase from about 16 at 1.38 bar to nearly 29 at 4.14 bar, highlighting the enhanced jet continuity as injection pressure rises.

When injection pressure increases, higher momentum of the fuel jet helps maintain continuous structure for longer durations, pushing the breakup region farther downstream. This phenomenon leads to formation of larger droplets due to extended breakup time. This relationship indicates that injection pressure can be adjusted to control the atomization process and droplet size distribution, thereby optimizing combustion performance in microturbine engines.

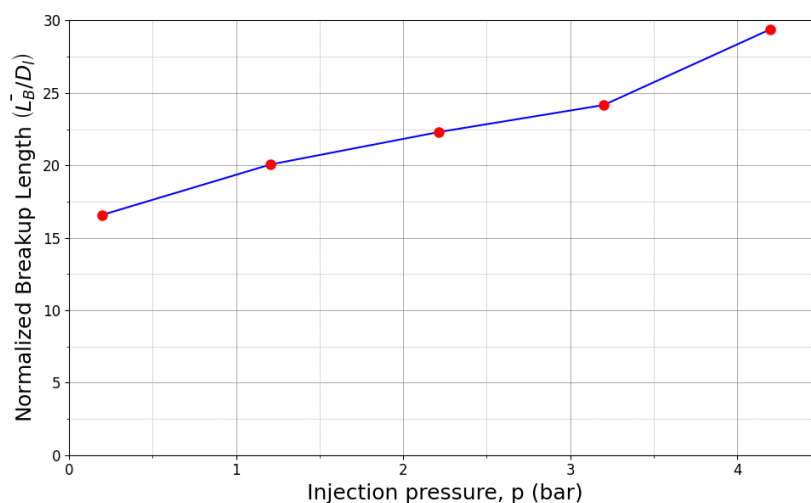
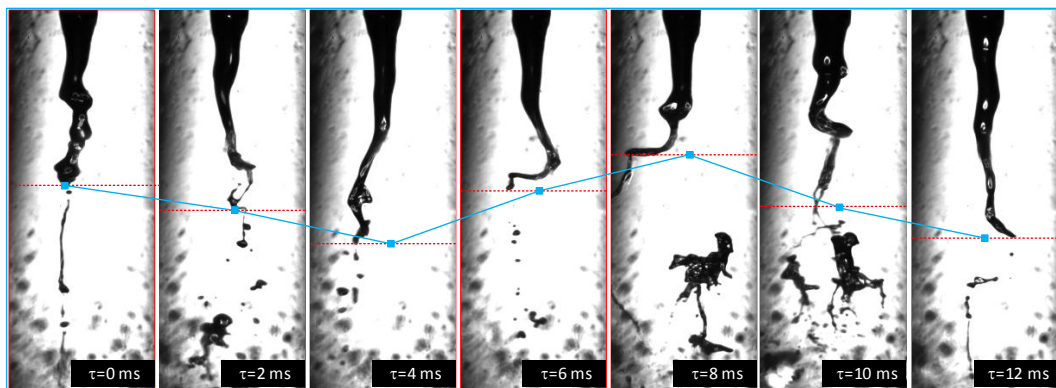


Fig. 11. Average breakup length vs. injection pressure.

The breakup process exhibits periodic oscillatory characteristics with alternating elongation and contraction phases of the liquid core (Fig. 12). This phenomenon is a manifestation of Rayleigh-Plateau instability at the gas-liquid interface, influenced by pressure fluctuations and interactions with the coaxial air flow. These oscillations contribute to creating diversity in droplet size and spatial distribution, directly affecting vaporization efficiency and combustion quality.



*Fig. 12. Flow evolution images of spray breakup in the vaporizer tube.*

Statistical analysis from thousands of high-speed images confirms the stability of the measurement method, with breakup length distribution concentrated around the mean value and low standard deviation. Standard error decreases progressively as sample size increases and stabilizes at  $\pm 0.01$  mm with 4000 images or more, demonstrating high reliability of the image processing algorithm in quantifying spray breakup characteristics.

In the initial phase of the study, water was used as the test fluid to calibrate the image processing algorithm and optimize the measurement system while ensuring operational safety. Although water offers advantages in terms of stability and parameter control, differences in physical properties compared to jet fuel - including viscosity (1.0 vs. 1.2-1.9 cP) and surface tension (73 vs. 25-30 mN/m) - may affect spray breakup characteristics. Room temperature conditions (25°C) also differ significantly from actual operating environments (300-500°C). After perfecting the measurement methodology, future research will apply the approach with actual fuel and high-temperature conditions to validate the algorithm's practical applicability.

## **5. Conclusions**

This study has successfully developed an integrated measurement system for spray breakup length in microturbine vaporizer tubes, comprising experimental setup that simulates operating conditions and an image processing algorithm combining

adaptive thresholding with Sobel edge detection. Results show that breakup length increases linearly from 3.2 to 6.8 mm as injection pressure increases from 1.38 to 4.14 bar, with characteristic periodic oscillations clearly observed.

The system achieves  $\pm 0.01$  mm accuracy with automated processing capability, enabling statistical analysis with over 4000 images per experimental condition. The algorithm is optimized for vaporizer tube environments, handling light refraction and density noise with  $> 95\%$  successful recognition rate. Implementation costs are 60% lower than advanced optical methods such as LIF, while processing time is reduced from several hours to several minutes per dataset. These characteristics enable application in vaporizer tube design optimization research with large data volumes.

The study used water as the test fluid instead of jet fuel, resulting in differences in viscosity and surface tension. Experiments were conducted at  $25^{\circ}\text{C}$  while actual operating conditions may reach  $300\text{-}500^{\circ}\text{C}$ . The current method only determines breakup length without measuring droplet size distribution or vaporization rates. Future research should employ actual fuel under high-temperature conditions to validate the practical applicability of the method in microturbines.

## References

- [1] J. Large and A. Pesyridis, "Investigation of micro gas turbine systems for high speed long loiter tactical unmanned air systems", *Aerospace*, Vol. 6, No. 5, 2019. DOI: 10.3390/aerospace6050055
- [2] G. Velidi and C. S. Yoo, "A review on flame stabilization technologies for UAV engine micro-meso scale combustors: Progress and challenges", *Energies*, Vol. 16, No. 9, 2023. DOI: 10.3390/en16093968
- [3] A. H. S. Weerakoon and M. Assadi, "Trends and advances in micro gas turbine technology for sustainable energy solutions: A detailed review", *Energy Conversion and Management: X*, Vol. 20, 2023. DOI: 10.1016/j.ecmx.2023.100483
- [4] I. A. Waitz, G. Gauba, and Y. S. Tzeng, "Combustors for micro-gas turbine engines", in *Proceedings of the ASME 1996 International Mechanical Engineering Congress and Exposition*. Atlanta, Georgia, USA, November 17-22, 1996, pp. 777-788, ASME. DOI: 10.1115/IMECE1996-0694
- [5] J. Anfossi, "*Innovation in micro gas turbines for aeronautical applications*", Ph.D. dissertation, University of London, 2024.
- [6] B. Chehroudi, S. Chen, F. Bracco, and Y. Onuma, "On the intact core of full-cone sprays", SAE Technical Paper 850126, 1985, pp. 764-773. DOI: 10.4271/850126

- [7] H. Eroglu, N. Chigier, and Z. Farago, "Coaxial atomizer liquid intact lengths", *Physics of Fluids*, Vol. 3, No. 2, pp. 303-308, 1991. DOI: 10.1063/1.858139
- [8] R. Woodward, R. Burch, K. K. Kuo, and F. B. Cheung, "Correlation of intact-liquid-core length for coaxial injectors", in *ICLASS 94 Proceedings of the Sixth International Conference on Liquid Atomization and Spray Systems*, 1994, Begell House.
- [9] T. D. Fansler and S. E. Parrish, "Spray measurement technology: A review", *Measurement Science and Technology*, Vol. 26, No. 1, 2014. DOI: 10.1088/0957-0233/26/1/012002
- [10] G. M. Faeth, L. P. Hsiang, and P. K. Wu, "Structure and breakup properties of sprays", *International Journal of Multiphase Flow*, Vol. 21, No. Supplement, pp. 99-127, 1995. DOI: 10.1016/0301-9322(95)00059-7
- [11] A. Kumar and S. Sahu, "Optical visualization and measurement of liquid jet core in a coaxial atomizer with annular swirling air", *Journal of Flow Visualization and Image Processing*, Vol. 25, Iss. 3-4, 2018. DOI: 10.1615/JFlowVisImageProc.2018027766
- [12] A. Moreira, A. Moita, and M. Panao, "Advances and challenges in explaining fuel spray impingement: How much of single droplet impact research is useful?", *Progress in Energy and Combustion Science*, Vol. 36, No. 5, pp. 554-580, 2010. DOI: 10.1016/j.pecs.2010.01.002
- [13] M. Sommerfeld and H. Qiu, "Experimental studies of spray evaporation in turbulent flow", *International Journal of Heat Fluid Flow*, Vol. 19, No. 1, pp. 10-22, 1998. DOI: 10.1016/S0142-727X(97)10002-9
- [14] A. H. Lefebvre and V. G. McDonell, *Atomization and Sprays*. CRC Press, 2017.
- [15] A. J. Yule and D. Salters, "A conductivity probe technique for investigating the breakup of diesel sprays", *Atomization Sprays*, Vol. 4, No. 1, 1994. DOI: 10.1615/AtomizSpr.v4.i1.20
- [16] W. Cai *et al.*, "Quantitative analysis of highly transient fuel sprays by time-resolved x-radiography", *Applied Physics Letters*, Vol. 83, No. 8, pp. 1671-1673, 2003. DOI: 10.1063/1.1604161
- [17] G. Charalampous, Y. Hardalupas, and A. Taylor, "Novel technique for measurements of continuous liquid jet core in an atomizer", *AIAA Journal*, Vol. 47, No. 11, pp. 2605-2615, 2009. DOI: 10.2514/1.40038
- [18] T. Acharya, *Image Processing - Principles and Applications*. Wiley-Interscience, 2005.
- [19] R. M. Haralick and L. G. Shapiro, "Image segmentation techniques", *Computer Vision, Graphics, Image Processing*, Vol. 29, No. 1, pp. 100-132, 1985. DOI: 10.1016/S0734-189X(85)90153-7
- [20] A. Saini and M. Biswas, "Object detection in underwater image by detecting edges using adaptive thresholding", in *2019 3rd International Conference on Trends in Electronics and Informatics (ICOEI)*, 2019, pp. 628-632, IEEE. DOI: 10.1109/ICOEI.2019.8862794

- [21] P. Roy, S. Dutta, N. Dey, and G. Dey, "Adaptive thresholding: A comparative study", in *2014 International Conference on Control, Instrumentation, Communication and Computational Technologies (ICCICCT)*, 2014, pp. 1182-1186, IEEE. DOI: 10.1109/ICCICCT.2014.6993140
- [22] D. Xiaoheng, L. Minghang, M. Jiashu, and W. Zhengyu, "Edge detection operator for underwater target image", in *2018 IEEE 3rd International Conference on Image, Vision and Computing (ICIVC)*, 2018, pp. 91-95, IEEE. DOI: 10.1109/ICIVC.2018.8492749
- [23] G. Singh, A. Kourmatzis, A. Gutteridge, and A. Masri, "Instability growth and fragment formation in air assisted atomization", *Journal of Fluid Mechanics*, Vol. 892, p. A29, 2020. DOI: 10.1017/jfm.2020.179
- [24] H. H. Nguyen, Q. Q. Nguyen, and X. P. Pham, "Design and operational evaluation of the combustion chamber of commercial Jetcat P130RX microturbine", in *Proceedings of the 2025 Conference on Information Technology, Electronics, Automation, and Space Science & Technology*. ISBN: 978-604-375-359-6.
- [25] G. B. García *et al.*, *Learning Image Processing with OpenCV*. Packt Publishing Birmingham (UK), 2015.

## NGHIÊN CỨU THỰC NGHIỆM VÀ ĐO CHIỀU DÀI PHÂN RÃ TIA PHUN DỰA TRÊN XỬ LÝ ẢNH TRONG ỐNG HÓA HƠI ĐỘNG CƠ TUA BIN KHÍ NHỎ

Nguyễn Hữu Hà<sup>1</sup>, Nguyễn Quốc Quân<sup>1</sup>, Phạm Xuân Phương<sup>1</sup>  
<sup>1</sup>*Viện Cơ khí động lực, Trường Đại học Kỹ thuật Lê Quý Đôn*

**Tóm tắt:** Việc đo chiều dài phân rã tia phun là yêu cầu then chốt nhằm tối ưu hóa thiết kế ống hóa hơi trong động cơ tua bin khí cỡ nhỏ. Chụp ảnh tốc độ cao hiện là một kỹ thuật đo lường hiện đại được sử dụng rộng rãi; tuy nhiên, khi áp dụng cho ống hóa hơi, kỹ thuật này đòi hỏi các thuật toán xử lý ảnh có độ chính xác cao để khắc phục hiện tượng khúc xạ ánh sáng qua thành ống thạch anh và nhiễu do biến thiên mật độ nhiên liệu. Nghiên cứu này phát triển một thuật toán kết hợp nhị phân hóa ngưỡng thích ứng với phát hiện biên Sobel, được tối ưu hóa cho điều kiện làm việc trong ống hóa hơi. Thí nghiệm được thực hiện ở các mức áp suất phun từ 1,38 đến 4,14 bar, với hơn 4000 ảnh được phân tích cho mỗi điều kiện nhằm đảm bảo độ tin cậy thống kê. Kết quả cho thấy chiều dài phân rã tăng từ 3,2 mm lên 6,8 mm khi áp suất phun tăng, đồng thời ghi nhận rõ ràng dao động chu kỳ của lõi tia. Thuật toán đạt được độ chính xác  $\pm 0,01$  mm với khả năng xử lý hoàn toàn tự động, qua đó cung cấp công cụ hiệu quả phục vụ nghiên cứu tối ưu hóa ống hóa hơi trong động cơ tua bin khí cỡ nhỏ.

**Từ khóa:** Ống hóa hơi; chiều dài phân rã; xử lý ảnh; toán tử Sobel; OpenCV.

Received: 05/08/2025; Revised: 29/09/2025; Accepted for publication: 12/12/2025

